Investigation of advanced data processing technique in magnetic anomaly detection systems

B. Ginzburg[(1)], A. Sheinker[(1)], L. Frumkis[(2)], B.Z. Kaplan[(2)], N. Salomonski[(1)]

[(1)] Soreq NRC, Yavne, 81800, Israel, borginz@soreq.gov.il

[(2)] Ben-Gurion University of the Negev, P.O. Box 653, Beer-Sheva, 84105, Israel

Abstract

Advanced methods of data processing in magnetic anomaly detection (MAD) systems are investigated. Raw signals of MAD based on component magnetic sensors are transformed into energy signals in the space of specially constructed orthonormalized functions. This procedure provides a considerable improvement of the SNR thus enabling reliable target detection. Estimation of the target parameters is implemented with the help of Genetic Algorithm. Numerous computer simulations show good algorithm convergence and acceptable accuracy in estimation of both target location and its magnetic moment.

Keywords: Magnetometer, Magnetic Anomaly Detection, Orthonormal Basis, Genetic Algorithm

1 Introduction

The necessity to detect hidden ferromagnetic objects (e.g. mines, underwater wrecks, and sunken ships etc) has led to several detection techniques, one of which is the Magnetic Anomaly Detection (MAD). The principle of the MAD is based on the ability to sense the anomaly in Earth magnetic field produced by the target. [1-3]

There are two basic types of MAD: search and alarm systems. In the first case, magnetic sensors are installed on the moving platform searching for hidden ferromagnetic target by surveying specific area along predefined paths (usually straight lines). Target presence is revealed as a spatial magnetic anomaly along the survey line passing in the vicinity of the target. MAD of alarm type makes use of stationary instruments producing an alarm signal when ferromagnetic target passes nearby the magnetic sensor. We assume the distance between the target and the sensor noticeably exceeding target dimensions so that target magnetic field is described by dipole model. MAD signal is time-depending magnetic field caused by mutual motion of magnetic dipole and the sensor. Therefore, our approach to signal processing is equally applicable for both types of MAD systems.

Magnetometers of various types are widely used for detection and characterization of hidden ferromagnetic objects by analyzing small Earth's magnetic field anomalies. The basic problem, which arises when measuring weak magnetic field anomalies, is a problem of small signal detection and estimation of target parameters in the presence of noise and interference.

In the present work we analyze different signal processing methods for MAD based on vector magnetic sensors. Our investigation covers two basic types of such sensors, where the first one (e.g. fluxgate) provides a direct reading of a field component and the second one (search coil in low-frequency mode) responds to time-derivative of magnetic field.

2 Presentation of field component signals with the aid of orthonormal functions

Let magnetic dipole whose moment components are M_x, M_y and M_z be located at the origin of the X, Y, Z coordinate system. The line of the sensor platform movement is parallel to the X axis. Each of three mutually orthogonal component sensors is aligned in parallel to one of the coordinate axes (Fig. 1).
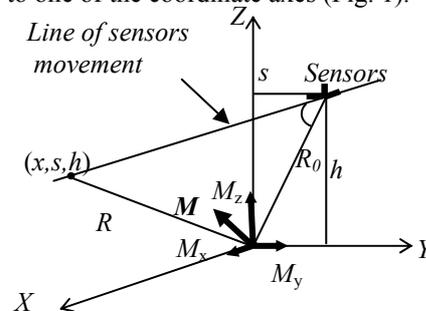

Figure 1. Relative position of the magnetic dipole M and the sensors.

The distance between the line of the sensor movement and the Z axis is s, and the distance between this line and the XY plane is h. R_0 is the distance between the dipole and the line of the sensor movement. It is the so-called CPA (closest proximity approach) distance,

$$R_0 = \sqrt{s^2 + h^2}. \qquad (1)$$

The magnetic field B generated by a point dipole with a moment M at some distance R from the dipole is

$$B = \frac{\mu_0}{4\pi} r^{-3} [3R^{-2}(M \cdot R)R - M] \qquad (2)$$

where $\mu_0 = 4\pi * 10^{-7}$ H/m is the permeability of free space.

Equation (2) can be rewritten in matrix form (see, for instance, [4])

$$\begin{vmatrix} B_x \\ B_y \\ B_z \end{vmatrix} = \frac{\mu_0}{4\pi R^5} \begin{vmatrix} 3x^2 - R^2 & 3xy & 3xz \\ 3yx & 3y^2 - R^2 & 3yz \\ 3zx & 3zy & 3z^2 - R^2 \end{vmatrix} \begin{vmatrix} M_x \\ M_y \\ M_z \end{vmatrix} \quad (3)$$

and after normalizing

$$w = x / R_0 \quad (4)$$

$$m_x = M_x / M, \ m_y = M_y / M, \ m_z = M_z / M, \quad (5)$$

$$M = \sqrt{M_x^2 + M_y^2 + M_z^2}$$

$$a_1 = 3s / R_0 \quad a_2 = 3h / R_0 \quad a_3 = 3s^2 / R_0^2 \quad (6)$$

$$a_4 = 3sh / R_0^2 \quad a_5 = 3h^2 / R_0^2$$

Equation (3) takes the form:

$$\begin{vmatrix} B_x \\ B_y \\ B_z \end{vmatrix} = \frac{\mu_0 M}{4\pi R_0^3} \begin{vmatrix} 3\varphi_4(w) - \varphi_1(w) & a_1\varphi_3(w) & a_2\varphi_3(w) \\ a_1\varphi_3(w) & a_3\varphi_2(w) - \varphi_1(w) & a_4\varphi_2(w) \\ a_2\varphi_3(w) & a_4\varphi_2(w) & a_5\varphi_2(w) - \varphi_1(w) \end{vmatrix} \begin{vmatrix} m_x \\ m_y \\ m_z \end{vmatrix} \quad (7)$$

where

$$\varphi_1(w) = (1+w^2)^{-1.5} \quad \varphi_2(w) = (1+w^2)^{-2.5} \quad (8)$$

$$\varphi_3(w) = w(1+w^2)^{-2.5} \quad \varphi_4(w) = w^2(1+w^2)^{-2.5}$$

Functions $\varphi_1(w)$, $\varphi_2(w)$ and $\varphi_3(w)$ are linearly independent, while $\varphi_4(w)$ can be excluded basing on

$$\varphi_4(w) = \varphi_1(w) - \varphi_2(w) \quad (9)$$

Applying Gram-Schmidt orthonormalization procedure [5] we get triplet of mutually orthogonal. functions $F_1(w)$, $F_2(w)$, and $F_3(w)$

$$F_1(w) = \sqrt{\frac{8}{3\pi}}(1+w^2)^{-1.5}$$

$$F_2(w) = \sqrt{\frac{384}{5\pi}}[(1+w^2)^{-2.5} - \frac{5}{6}(1+w^2)^{-1.5}] \quad (10)$$

$$F_3(w) = \sqrt{\frac{128}{5\pi}}w(1+w^2)^{-2.5}$$

satisfying the usual orthonormalization conditions:

$$\int_{-\infty}^{+\infty} F_i(w)F_j(w)dw = 0 \qquad \text{for } i \ne j, \text{ and}$$

$$i, j = 1, 2, 3. \quad (11)$$

$$\int_{-\infty}^{+\infty} F_j^2(w)dw = 1$$

The orthonormal functions $F_1(w)$, $F_2(w)$, and $F_3(w)$ are shown in Fig. 2
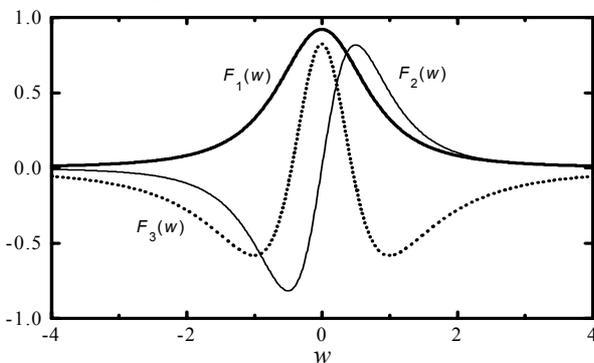

Figure 2. The set of orthonormal functions:
$F_1(w)$, $F_2(w)$, and $F_3(w)$ for presentation
of field component signals.

The field components (7) as a function of sensor platform movement can now be expressed as a linear combination of basis functions $F_i(w)$

$$\begin{vmatrix} B_x \\ B_y \\ B_z \end{vmatrix} = \overline{A} \cdot \begin{vmatrix} F_1 \\ F_2 \\ F_3 \end{vmatrix} \quad (12)$$

where $\overline{A}$ is 3x3 matrix which coefficients depend on a particular dipole position and orientation and can be obtained in the following way:

$$A_{ij} = \int_{-\infty}^{\infty} F_i(w)B_j(w)dw \quad i=1, 2, 3; j=x, y, z \quad (13)$$

It is important to underline that (12, 13) are correct not only for any dipole position and orientation but for any direction of sensor platform and its orientation as well. This gives us an opportunity to implement a unified algorithm for processing of MAD signal as it will be shown below.

It is worthy to note that basic functions (10) coincide with the same functions which can be employed for the case of MAD based on scalar magnetometer [6, 7].

3 Presentation of time derivatives of field component with the aid of orthonormal functions

Search-coil magnetometers are widely used for component measurements in MAD systems. For direct mode of operation the output signal of search-coil magnetometer is proportional to the ambient field. For that case all results of previous section are applicable. The direct mode of operation is usually a result of relatively large self capacitance of the coil windings, and/or electronics correction measures. However, in the lower part of operation frequency band search coil sensor operates in derivative mode [8]. In this case sensor signals $S_{x,y,z}$ can be written as

$$S_{x,y,z} = K\frac{dB_{x,y,z}}{dt} = K\frac{dB_{x,y,z}}{dw}\frac{dw}{dx}\frac{dx}{dt} = K\frac{V}{R_0}\frac{dB_{x,y,z}}{dw} \quad (14)$$

562

where K is coefficient depending on permeability of search-coil core, number of turns, and coil geometry, while V is the velocity of the sensor platform. Implementing mathematical transformations like in previous section it is easy to show that signals of search-coil magnetometers (14) can be presented by linear combination of four functions

$$\psi_1(w) = w(1 + w^2)^{-2.5},$$

$$\psi_2(w) = w(1 + w^2)^{-3.5}, \quad \psi_3(w) = (1 + w^2)^{-3.5},$$

$$\psi_4(w) = w^2(1 + w^2)^{-3.5} \quad (15)$$

After implementation of Gram-Schmidt procedure we get quartet of mutually orthogonal. functions:

$$v_1(w) = \sqrt{\frac{1024}{7\pi}}\psi_4(w), \quad v_2(w) = \sqrt{\frac{1024}{21\pi}}\psi_2(w),$$

$$v_3(w) = \sqrt{\frac{128}{21\pi}}(\psi_3(w) - 3\psi_4(w)),$$

$$v_4(w) = \sqrt{\frac{384}{\pi}}(\psi_1(w) - \frac{4}{3}\psi_2(w)). \quad (16)$$

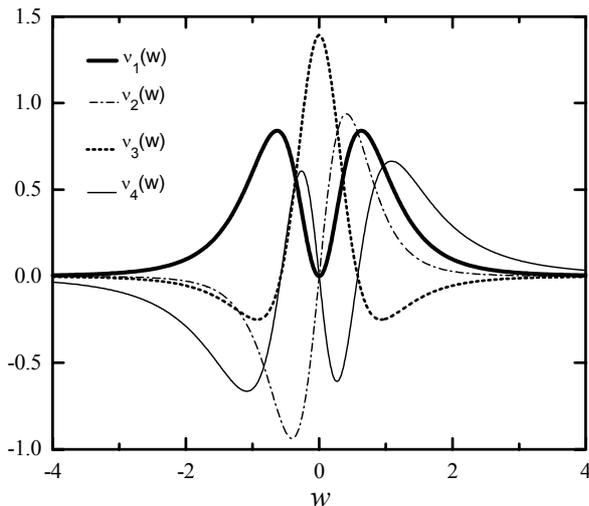The orthonormal functions $v_1(w)$, $v_2(w)$, $v_3(w)$, and $v_4(w)$ are shown in Fig. 3

Fig. 3. The set of orthonormal functions: $v_1(w)$, $v_2(w)$, $v_3(w)$, and $v_4(w)$ for presentation of time derivatives of field component signals.

Now the vector of time derivatives $d\mathbf{B}/dw=(dB_x/dw, dB_y/dw, dB_z/dw)$ can be written in matrix form as

$$\begin{vmatrix} \dfrac{dB_x}{dw} \\ \dfrac{dB_y}{dw} \\ \dfrac{dB_z}{dw} \end{vmatrix} = \overline{D} \begin{vmatrix} v_1(w) \\ v_2(w) \\ v_3(w) \\ v_4(w) \end{vmatrix} \quad (17)$$

where $\overline{D}$ is 3x4 matrix which coefficients are expressed similar to (13)

$$D_{ij} = \int_{-\infty}^{\infty} F_i(w)B_j(w)dw \quad i=1, 2, 3, 4 \quad j=x, y, z \quad (18)$$

4 Employment of the orthonormal functions for enhancement of signal to noise ratio

Decomposition of the sensor signal in the space of orthonormal basis (10) or (16) provides us with an effective way for enhancement of signal to noise ratio. Following [6,7] we construct a criterion function E for primary detection algorithm as

$$E_j = A_{1j}^2 + A_{2j}^2 + A_{3j}^2 \quad j=x, y, z \quad (19)$$

for the sensors which signals are proportional to field components and

$$E_j = D_{1j}^2 + D_{2j}^2 + D_{3j}^2 + D_{4j}^2 \quad j=x, y, z \quad (20)$$

These expressions can be interpreted as the energy of the signal in the space of chosen basis. Coefficients in (19, 20) are calculated as convolutions of the raw signal of the sensor with appropriate basic functions for each point w_0 of the sensor platform track.

$$A_{i,j}(w_0) = \int_{-\infty}^{+\infty} F_i(w + w_0)\widetilde{B}_j(w)dw$$
$$i=1, 2, 3; j=x, y, z \quad (21)$$

$$D_{i,j}(w_0) = \int_{-\infty}^{+\infty} v_i(w + w_0)\widetilde{S}_j(w)dw$$
$$i=1, 2, 3,4 \quad j=x, y, z \quad (22)$$

In practice integration in (21, 22) is confined within finite "observation window" (integration limits) which length is chosen basing on the expected value of CPA so to enable real-time detection scheme.

An example of application of given algorithm for target detection is shown in Fig. 4. Raw data acquired by Z-fluxgate (Fig. 4a) contain bell-shaped dipole signal (m_x=0.27, m_y=0.53, m_z=0.8) with SNR equal to 0.4. Data processing according to (19, 21) (Fig. 4b) increases SNR up to 12 which is much better than simple band-pass filtering (Fig 4c). It is a consequence of the principle of algorithm (19 -22) which is based on prior guess of magnetic dipole structure of the target signal.

5 Problem of target localization and estimation of its magnetic moment

Aforementioned algorithm provides effective tool for target detection. However, it does not permit acceptable estimation of the target location and its magnetic moment.

Aiming to advance the subject of target parameters estimation we have proposed and analyzed application of Genetic Algorithm (GA). To start with it, let us first note that in practice magnetic measurements are performed in a sequentially discrete manner while the magnetometer moves along the track.

By taking N samples of the measured magnetic field $\vec{B}(1), \vec{B}(2),...\vec{B}(N)$ we get a nonlinear over-determined set of equations (for large enough N),
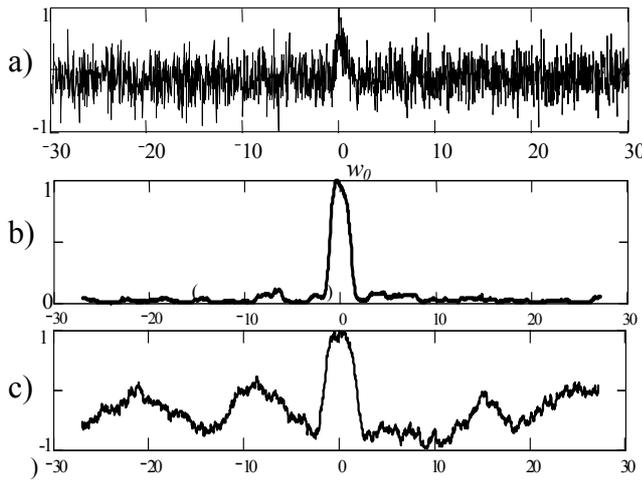
Fig. 4. Illustration of the data processing algorithm:
a) raw signal sensed by the Z-fluxgate,
b) energy calculated according to (19, 21),
c) The raw signal after a band pass filter

$$\begin{cases} \vec{B}(1) = \vec{B}(\vec{m}, \vec{r}) \\ \vec{B}(2) = \vec{B}(\vec{m}, \vec{r} + \Delta\vec{r}_2) \\ \dots\dots\dots\dots \\ \vec{B}(N) = \vec{B}(\vec{m}, \vec{r} + \Delta\vec{r}_N) \end{cases} \quad (23)$$

We aim to solve equation (23) for $\vec{m}$ and $\vec{r}$, which are the target magnetic moment, and the vector from the target to the first sample point respectively. The displacements $\Delta\vec{r}_2, \Delta\vec{r}_3 \dots \Delta\vec{r}_N$ are the vectors from the position of the first sample to the position of samples 2,3,. . .,N respectively. These displacements can be measured precisely using advanced navigation systems and therefore are considered as known. Solving equation (23) analytically is not trivial especially in the presence of noise. That is why we have divided the problem domain into cells of predetermined resolution.

Each of the vectors $\vec{m}$ and $\vec{r}$, consists of three Cartesian components, Hence, one can define a single six element solution vector,

$$\vec{X} = (\vec{m}, \vec{r}) = (m_x, m_y, m_z, r_x, r_y, r_z)^T \quad (24)$$

For each component of $\vec{m}$ and $\vec{r}$ there should be set a range according to practical considerations concerning target possible location and magnetic dipole range. Then, for each component of $\vec{m}$ and $\vec{r}$ there should be defined a resolution according to the needed accuracy. A short example illustrates the process. Consider a search for a target, whose magnetic moment ranges from -1 Am^2 to +1 Am^2. The needed accuracy for estimating the target magnetic field is 0.02 Am^2. Assume that the search takes place in a cube with a side length of 2 m, and we would like to localize target with accuracy of 2 cm. For each element of the solution vector $\vec{X}$,

there are 100 possibilities, resulting in a finite solution space of a total 100^6 possible solutions, from which we have to choose the nearest to actual one. As we see the problem becomes that of searching the (sub) optimal solution out of a finite solution space instead of solving equation (23) analytically. The limited range of possible solutions and the restricted resolution result in sub optimal solutions rather than optimal, that is, however, acceptable for many applications.

Checking all possible solutions one by one would consume enormous time, which is not available in real time systems. For this reason we propose the Genetic Algorithm as a rapid search method.

6 Application of Genetic Algorithm for target localization and estimation of its magnetic moment

Genetic algorithms provide an effective way to solve problems such as traveling salesman (the shortest route to visit a list of cities) [9]. In this work we focus on GA as a search method to find the maximum of an object function, also called fitness function. The GA mimics the evolutionary principle by employing three main operators: selection, crossover, and mutation. As a first step we build a chromosome, which has the genotype of the desired solution. In the case of localization of a magnetic dipole, the chromosome has the form of (24). Each element of the chromosome is called gene and may take only restricted values that were defined previously by range and resolution as is explained in the former example. Implementing the evolutionary principle obligates a collection of L chromosomes, which is entitled as population. At first, random values are set for each chromosome of the population. A fitness value is calculated for each chromosome by substituting for the chromosome into the fitness function. The chromosomes can be arranged in a list from the fittest chromosome (with the largest fitness result) to the least fit one. Then the selection operator is applied, selecting only the K fittest chromosomes from the list. There are several ways to perform the selection, which would not be described here. After selection, the crossover operator is utilized resembling a natural breeding action. Only the K fittest chromosomes of the list are allowed to breed amongst themselves by the following mathematical operation,

$$\vec{X}_{new} = \lambda\vec{X}_i + (1 - \lambda)\vec{X}_j \quad (25)$$

Chromosomes $\vec{X}_i, \vec{X}_j$ are randomly chosen from the list of the K fittest chromosomes. λ is a crossover parameter (usually 0.5), and $\vec{X}_{new}$ is a newborn chromosome. The process is repeated until a population of K newborn chromosomes is reached. Afterward mutation operator is implemented by randomly selecting a chromosome from the newborn population, and changing a random gene to a random

permitted value. The randomness property enables the GA to overcome local minima. After mutation is applied, fitness evaluation is performed on the mutated newborn population. The process of fitness evaluation-selection-crossover- mutation is repeated for a predetermined number of generations or until the fittest chromosome reaches a predefined fitness value. The convergence of the GA is expressed by increase in the average fitness of the population from generation to generation. The chromosome with the largest fitness value is chosen as the solution, according to 'survival of the fittest' principle. Defining an appropriate fitness function is an important step in utilizing GA. We have proposed the following fitness function for magnetic dipole localization by a 3-axis magnetometer (without considering noise characteristics):

$$fitness(\vec{X}_j) = -\sum_{n=1}^{N} \frac{[B_x(n) - B_x(\vec{X}_j)]^2 + [B_y(n) - B_y(\vec{X}_j)]^2 + [B_z(n) - B_z(\vec{X}_j)]^2}{B_x^2(n) + B_y^2(n) + B_z^2(n)} \tag{26}$$

where $B_{x,y,z}(n)$ represents the n-th measurement sample while $B_{x,y,z}(\vec{X}_j)$ is calculated magnetic field produced by chromosome j. Note that the fittest chromosome fitness value is closest to zero.

In order to investigate magnetic dipole localization by Genetic Algorithm, we performed numerous computer simulations. To illustrate some of simulation results we have chosen magnetic dipole with $M_x = 0.27$ A·m^2, $M_y = 0.53$ A·m^2, $M_z = 0.8$ A·m^2 located at the origin of coordinate system (0,0,0). The samples were taken every 0.1 m from -7.1m to +7.1m along the x-axis (south-north) at a constant y-axis coordinate of s=6.7 m (see Fig. 1) and a constant height h=2.4 m. This results in a CPA distance of R_0= 7 m. Random noise was added to the magnetic dipole signal to ensure SNR of 0.4 (Fig. 4a). The GA was set to a population of 100 chromosomes and a stop condition of 10,000 generations. The mutation probability was set to 5% and the crossover probability to 30%. Statistical processing of the simulation results after 100 executions leads to the following results.

Moment estimation
Total magnetic moment of the target dipole is 1 A·m^2. Estimated magnetic moment averaged over 100 executions of GA algorithm was 1.1 A·m^2 – relative biased estimate value of 10%. Statistical distribution of the obtained moment values is shown in Fig. 5.

Target localization
Estimated target location averaged over 100 executions of GA algorithm was (-0.26m, -0.45m, 0.07m) so that absolute biased estimate length was 0.53m which makes up less than10% error relative to CPA distance. Spatial distribution of the obtained target locations is shown in Fig. 6.

7 Conclusion

In the present work we have investigated two approaches to the data processing of the MAD signals.
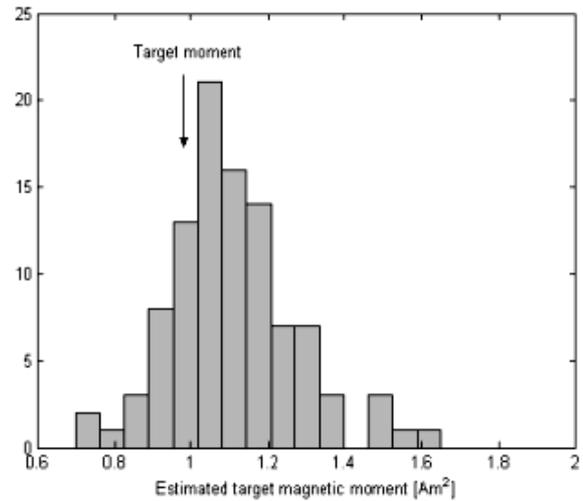

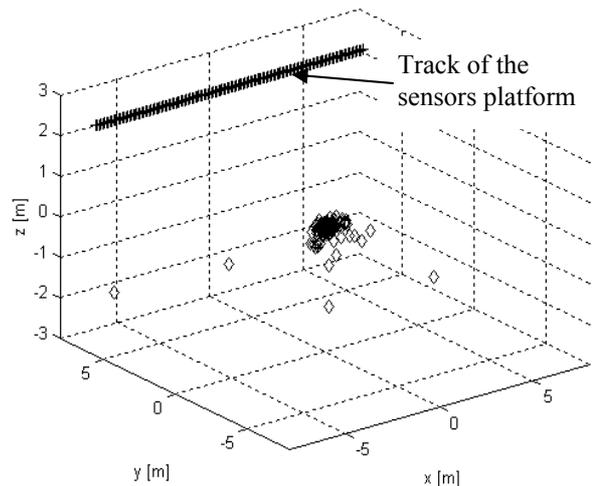Fig. 5 Distribution of magnetic moments obtained as a result of 100 GA algorithm executions.

Fig. 6 Spatial distribution of target locations obtained as a result of 100 GA algorithm executions.

Our first approach to MAD signal processing relies on the decomposition of the MAD signal in the space of specially constructed orthonormalized functions. It turns out that the signals of fluxgate sensor can be

presented as a linear combination of three orthonormal functions while the search coil signals need four orthonormal functions for correct representation. The dipole energy signal is introduced in the basis chosen and is found to be a useful function for the data processing algorithm based upon the results of the modeling. It is important to underline that this method works equally well for various orientations of target moment relative to external Earth's magnetic field and direction of survey line. The aforementioned processing procedure provides a considerable improvement of the SNR thus enabling reliable target detection even with low values of SNR.

To proceed with target parameters estimation we proposed and tested another approach to MAD signal processing based on Genetic Algorithm. Typical parameters of GA included: population of 100 chromosomes; stop condition of 10,000 generations; mutation probability 5%; crossover probability 30%. Statistical processing of the simulation results after 100 executions shows good algorithm convergence and acceptable (<10%) relative errors of main target parameters estimation even with rather low signal-to-noise ratio in raw magnetometer signal.

8 References

[1] M. Hirota, T. Furuse, K. Ebana, H. Kubo, K. Tsushima, T. Inaba, A. Shima, M. Fujinuma and N. Tojyo, "Magnetic detection of a surface ship by an airborne LTS SQUID MAD", *IEEE Trans. Appl. Supercond*. 11 pp 884-887 (2001) p.560

[2] W.M. Winn, in: C. E. Baum (Ed.), *Detection and Identification of Visually Obscured Targets*, Taylor and Francis, Philadelphia, PA, (1999), Chapter 11, pp 337-376.

[3] H. Zafrir, N. Salomonski, Y. Bregman, B. Ginzburg, Z. Zalevsky, M. Baram, "Marine magnetic system for high resolution and real time detection and mapping of ferrous submerged UXO, sunken vessels, and aircraft", in: *Proc. UXO/Countermine Forum 2001*, New Orleans, LA, 9-12 April 2001.

[4] R. B .Semevsky, V. V. Averkiev, V. V. Yarotsky, *Special Magnetometry*, "Nauka", St.-Petersburg, (2002), pp.228, (in Russian)

[5] G.A. Korn, T.M. Korn, *Mathematical Handbook for Scientists and Engineers*, McGraw Hill, New York, 2nd ed., (1968), p. 491.

[6] Y. D. Dolinsky, "Vliyanie osobennostei signala na strukturu optimalnogo priemnika pri obnaruzhenii namagnichennykh tel", *Geofizicheskaya Apparatura*, 97 pp 29-38 (1993) (in Russian).

[7] B. Ginzburg, L. Frumkis and B.Z. Kaplan, "Processing of magnetic scalar magnetometer signals using orthonormal functions", *Sens. Actuators* A 102, pp 67-75 (2002).

[8] H. C. Seran, P. Fergeau, "An optimized low-frequency three-axis search coil magnetometer for space research", *Review of Sci. Instr.*, 76, pp 044502-1 - 044502-10 (2005)

[9] F. O. Karray, C. DeSilva *Soft Computing and Intelligent Systems Design Theory, Tools and Applications,* Addison Wesley, England, (2004),